Human Pathology (2019) **86**, 233–242

ELSEVIER

Human PATHOLOGY

www.elsevier.com/locate/humpath

Original contribution

Paip1 predicts poor prognosis and promotes tumor progression through AKT/GSK-3β pathway in lung adenocarcinoma☆,☆☆

Yixuan Wang MD, Junjie Piao MD, Qianrong Wang MD, Xuelian Cui MD, Ziqi Meng MD, Tiefeng Jin MD, PhD*, Zhenhua Lin MD, PhD*

Department of Pathology and Cancer Research Center, Yanbian University Medical College, Yanji 133002, China
Key Laboratory of the Science and Technology Department of Jilin Province, Yanji 133002, China

Received 29 August 2018; revised 12 November 2018; accepted 16 November 2018

Keywords:
Lung adenocarcinoma;
Polyadenylate-binding protein-interacting protein 1;
Prognosis;
Proliferation;
Migration

Summary The expression and biological function of Paip1 remain poorly understood in most human cancers. The objective of this research is to investigate its clinical significance and roles in lung adenocarcinoma (LADC). Immunohistochemistry was used to determine Paip1 expression in 58 cases of LADC patients with strict follow-up and 60 cases of adjacent normal lung tissues. Paip1 protein was upregulated in 77.6% (45/58) LADC tissues compared with adjacent normal lung tissues. The overexpression of Paip1 was significantly correlated with histologic grade, clinical stage, and poor prognosis. Small interfering RNA–mediated transfection was performed in A549 and H1299 cells. Paip1 depletion attenuated the proliferation and migration of A549 and H1299 cells. Paip1 also changed the expression of epithelial-to-mesenchymal transition markers including E-cadherin, Vimentin, Slug, and Snail. Furthermore, Paip1 regulated AKT/GSK-3β oncogenic signaling pathways. In conclusions, Paip1 expression is frequently upregulated in LADC, and its overexpression correlates with poor prognosis in LADC patients. Attenuated Paip1 expression suppresses proliferation and epithelial-to-mesenchymal transition–related migration of A549 and H1299 cells by regulating the AKT/GSK-3β signaling pathway.

1. Introduction

Currently, lung cancer is the most common malignancy and the leading cause of cancer death around the world; its incidence is increasing especially in China [1,2]. Lung cancer arises from the cells of the respiratory epithelium. Based on histology, there are 2 primary types of lung cancer: non–small cell lung cancer (NSCLC) and small cell lung cancer. Approximately 85% of primary lung cancers are NSCLC, which includes lung adenocarcinoma (LADC) and squamous cell carcinoma [3]. Adenocarcinoma by itself accounts for 38.5% of all lung cancer cases [4]. Metastasis of LADC is the main

☆ Competing interests: The authors declare that they have no competing interests.

☆☆ Funding/Support: This research was supported by the National Natural Science Funds of China (Nos. 31760313 and 81660394), the funds of Changbai Mountain Scholar Project, and Key Laboratory of the Science and Technology Department of Jilin Province (No. 20170622007JC).

* Corresponding authors at: Department of Pathology and Cancer Research Center, Yanbian University Medical College, No. 977, Gongyuan Rd, Yanji 133002, China.
E-mail addresses: jintf@ybu.edu.cn (T. Jin), zhlin720@ybu.edu.cn (Z. Lin).

https://doi.org/10.1016/j.humpath.2018.11.017
0046-8177/

cause of cancer treatment failure and poor prognosis [5]. However, the complicated molecular and cellular mechanisms involved in LADC metastasis remain poorly understood. Therefore, elucidation of the mechanisms underlying the pathogenesis of LADC is important to identify effective prognostic and therapeutic biomarkers for this lethal disease.

Polyadenylate-binding protein-interacting protein 1 (Paip1) is a protein that encoded by the *PAIP1* gene, which located in 5p12 [6]. Human Paip1 was originally described as a ~70-kDa protein and discovered as a PABP-binding protein that stimulates translation of luciferase reporter messenger RNA (mRNA) in COS-7 cells [7]. Previous studies have reported that ternary complexes composed of Paip1-PABP-eIF4G and Paip1-eIF3-eIF4G can form in vitro, which brings about the circularization of the mRNA and promotes translation initiation [8]. Paip1 also was involved in the control of cell growth, proliferation, and differentiation. It was overexpressed in invasive cervical cancers and in amyotrophic lateral sclerosis [9,10]. Recent research has reported that overexpression of Paip1 protein was related to the overall survival of breast cancer patients and affected breast cancer cell growth [11]. However, the pathogenic role of Paip1 in LADC has not yet been reported.

In this study, we firstly investigated the correlation between the expression of Paip1 and clinicopathological parameters of LADC patients and evaluated its prognostic value. Finally, the function of Paip1 and possible molecular mechanism in A549 and H1299 lung cancer cells were elucidated.

2. Materials and methods

2.1. Ethics statement

This research was approved by the Ethical Committee of Yanbian University Medical College in China and was conducted in compliance with the tenets of the Declaration of Helsinki. Informed consent was obtained from all participants before the analysis. Follow-up survival data were collected retrospectively through medical record analyses.

2.2. Oncomine analysis

Oncomine Cancer Microarray database (http://www.oncomine.org) was queried to study gene expression of Paip1 in LADC cancer samples. A set of public and published microarray data were used to analyze the Paip1 mRNA level between the LADC and normal lung tissues, using "LADC," "Paip1," and "mRNA" as terms for searching the objective data.

2.3. Clinical samples

To determine the clinical and prognostic significance of Paip1 in LADC, 58 LADC tissues and 60 adjacent normal lung tissues were used for this study, along with complete clinicopathological and survival data. These tumors were randomly obtained from the Tumor Tissue Bank of Yanbian University Medical College between 2008 and 2013. All samples were formalin-fixed, paraffin-embedded blocks, which were then cut into 4-μm-thick sections. Clinicopathological clinical TNM stages were determined according to the Staging Manual of the American Joint Committee on Cancer, seventh edition [12]. Clinical information of the samples is summarized in Tables 1 and 2. None of the patients received any adjuvant chemotherapy before lung cancer surgery resection. The 58 LADC patients had been followed up for 7 years or until death. In this study, in 60 cases, adjacent normal lung tissues were collected from the cancer resection margin.

2.4. Immunohistochemistry staining analysis

Immunohistochemistry (IHC) analysis was performed using the Dako LSAB kit (Dako, Glostrup, Denmark). Briefly, to avoid endogenous peroxidase activity, sections of paraffin-embedded specimens were dewaxed with xylene and rehydrated through a graded series of ethanol. The antigen was retrieved, and the slides were incubated with the Paip1 antibody (1:200 dilution, no. 10675-1-AP; Proteintech, Rosemont, IL) overnight at 4°C . Then, the sections were incubated with the secondary antibody for 30 minutes. Diaminobenzidine-hydrogen peroxide was the chromogen, and 0.5% hematoxylin was used for counterstaining. Then we used a rabbit IgG isotype control, which showed negative staining. The positive tissue sections were processed without the primary antibody to serve as another negative control.

Two pathologists who did not possess knowledge of the clinical data examined and scored all tissues specimens. In the case of a discrepancy, a final score was established by reassessment by both pathologists using a double-headed microscope. A cytoplasmic expression pattern was considered positive staining. Briefly,

Table 1 Paip1 protein expression in LADC

Diagnosis	No. of cases	Paip1				Positive case rate (%)	Strong positive case rate (%)
		−	+	++	+++		
Adjacent normal lung	60	48	10	2	0	20.0	3.3
Lung adenocarcinoma	58	13	18	14	13	77.6 *	46.6 *

NOTE. Positive rate: percentage of positive cases with +, ++, and +++ staining score. Strongly positive rate: percentage of positive cases with ++ and +++ staining score.

* $P < .01$ compared with adjacent normal lung tissues.

Table 2 Relationship between Paip1 protein overexpression and the clinicopathological parameters of LADC

Variables	No. of cases (*n*)	Paip1, strong positive rate, n (%)	χ^2	*P*
Sex				
Male	36	15 (41.7)	0.910	.340
Female	22	12 (54.5)		
Age (y)				
>62	29	15 (51.7)	0.624	.430
≤62	29	12 (41.4)		
Tumor size (cm)				
≤4	41	19 (46.3)	0.002	.960
>4	17	8 (47.1)		
Histologic grade				
Grade 1	4	1 (25.0)	8.188	.017 *
Grade 2	31	10 (32.3)		
Grade 3	23	16 (69.6)		
Clinical stage				
I + II	43	16 (37.2)	5.832	.016 *
III + IV	15	11 (73.3)		
Lymph node status				
N0	37	16 (43.2)	0.450	.503
N+	21	11 (52.4)		

* $P < .05$.

staining intensity of tissue sections scored as follows: 0, no staining; 1, definite but weak staining; and 2 and 3, moderate and intense staining of Paip1. The staining area was scored as follows: scored as 0 (negative, no or less than 5% positive cells), 1 (5%-25% positive cells), 2 (26%-50% positive cells), 3 (51%-75% positive cells), and 4 (>75% positive cells). The total scores were divided into low or high expression groups by multiplying the intensity score and the proportion of positive cells score, ranging from 0 to 12. Zero marked as −; 1 to 3 points, +; 4 to 6 points, ++; and 8 to 12 points, +++. For survival analysis, −, + scored samples were considered as low Paip1 expression, and ++, +++ scored samples were considered as high Paip1 expression.

2.5. Cell lines and cell culture

The human lung cancer cell lines A549, H1975, H1944, and H1299 were obtained from the American Type Culture Collection (ATCC, Manassas, VA). The H1299 cell line is derived from a human large cell lung carcinoma [13]. All cell lines were routinely grown in Dulbecco modified Eagle medium and RPMI-1640 media (Gibco, Gaithersburg, MD), which were supplemented with 10% fetal bovine serum (FBS) and 1% penicillin/streptomycin in a 5% CO_2 humidified incubator at 37°C.

2.6. Small interfering RNA transfection

Small interfering RNA (siRNA) targeting Paip1 and control siRNA were synthesized by RiboBio (Guangzhou, China). Cells were seeded into 6-well plates and then cultured to 70% to 80% confluence. After 24 hours, cells were transfected with 50 nM Paip1 or control siRNA using lipofectamine 3000 (Invitrogen, Carlsbad, CA) according to the manufacturer's instructions. According to the silencing effects of Paip1, siRNA3 and control siRNA were used in this study. The sequence of siRNA3 was 5′-CTGACAATTAGCCCACAGA-3′.

2.7. Cell viability assay

Cells were seeded into 96-well plates (5000 cells). Each wells medium was removed and replaced by 20 μL of 5 mg/mL MTT in 1% FBS-containing medium, and cells were incubated in the CO_2 incubator at 37°C for 4 hours. The medium was removed from each well, and the reduced MTT dye was dissolved in 100 μL dimethyl sulfoxide was added to the well. Absorbance at 570 nm was determined using a microplate reader (Tecan Infinite M200; Tecan, Switzerland).

2.8. Colony formation assay

Cells were transfected for 48 hours and seeded in 6-well plates (1000 cells). The cells were incubated for 2 weeks. Colonies were fixed with methanol and then stained with Giemsa. The number of colonies with more than 50 cells was counted. The colonies were manually counted using a microscope (BX53, Olympus, Tokyo, Japan).

2.9. EdU proliferation assay

The EdU assay was conducted using a Cell-Light EdU DNA Cell Proliferation Kit (RiboBio). Briefly, 50 μM EdU labeling medium was added to the cell culture to allow for incubation for 2 hours at 37°C under 5% CO_2. Afterward, cells was fixed with 4% paraformaldehyde followed by staining

with Apollo Dye Solution and then mounted with Hoechst 33342. The positive cells were photographed and counted using a fluorescence microscope (IX53; Olympus).

2.10. Wound healing assay

Cell monolayers (80% confluence) were scratched using a 200-μL pipette tip to create a narrow wound-like gap. The wounded monolayer was photographed at 0 and 24 hours under a Nikon Eclipse TE300 microscope (Leica, Jena, Germany), respectively.

2.11. Migration assay

The migration assay used 24-well plates with 8-μm transwell inserts (Millipore, Billerica, MA). Cells were seeded into the upper insert in serum-free media, whereas media containing 10% FBS was added to the lower insert as a chemoattractant for 24 hours. The cells on the upper filter surface were removed, and cells on the lower filter surface were fixed with ethanol and stained with Giemsa. The images were taken with a BX53 Olympus microscope, and the number of cells in 3 to 5 fields was counted.

2.12. Immunofluorescence staining

Cells were grown on glass coverslips and fixed with 4% paraformaldehyde for 10 minutes, permeabilized with 0.5% TritonX-100 (CWBIO, Beijing, China) and blocked with 3% Albumin Bovine V (Solarbio, Beijing, China) for 1 hour. Cells were then incubated with the primary antibody at 4°C overnight, followed by incubation with a fluorescent-labeled secondary antibody for 1 hour. After washing with PBS, cells were counterstained with DAPI (Beyotime, Haimen, China), and the coverslips were mounted with Antifade Mounting Medium (Beyotime). Imaging was performed using a BX53 Olympus microscope.

2.13. Western blot analysis

Cells were lysed in RIPA buffer containing protease inhibitor cocktail and phosphatase inhibitor cocktail. The total protein samples (30 μg), quantified with a BCA protein assay (Pierce, Rockford, IL), were separated through 8% to 10% SDS-PAGE and transferred to PVDF membranes (Millipore, Darmstadt). The membranes were blocked with a 5% skim milk solution and subsequently incubated with the primary antibody Paip1, Akt, p-Akt (Proteintech), glycogen synthase kinase-3β (GSK-3β), p-GSK-3β, Snail, Slug (Cell Signaling, Danvers, MA), E-cadherin (Abcam, Cambridge, MA), Vimentin (Millipore, Darmstadt), and β-actin (Zhongshan, Beijing, China) for overnight at 4°C. After incubation with secondary antibody dilution of 1:3000 for 2 hours, the bands were visualized with Chemi Doc Touch Imaging System (Bio-Rad, Hercules, CA).

2.14. Statistical methods

All statistical analyses were analyzed using the SPSS17.0 software (Chicago, IL). Fisher exact test and the χ^2 test were used to compare the variables between groups. Kaplan-Meier analysis was used to compare the survival rates among groups. Data were presented as the mean ± SD and examined for their statistical significance of difference using 1-way analysis of variance and t test. All experiments were carried out at least 3 times. $P < .05$ was considered statistically significant.

3. Results

3.1. Paip1 is significantly upregulated in LADC and positively correlates with poor prognosis in LADC patients

Initially, analysis of the microarray datasets in Oncomine Database indicated that the mRNA level of Paip1 in LADC was significantly higher than that in normal lung tissues (Fig. 1A). Next, we performed IHC staining analysis the expression of Paip1 in 58 LADC tissues and 60 adjacent normal lung tissues. As shown in Fig. 1B-I, Paip1 was predominantly located in the cytoplasm of cancer cells and remarkably elevated in LADC tissues. The positive rate of Paip1 protein expression was 77.6% (45/58) in LADC tissues, which was significantly higher than that in adjacent normal lung tissues (20.0% [12/60]; $P < .01$). Similarly, the strongly positive rate of Paip1 protein expression (46.6% [27/58]) in LADC tissues was also significantly higher than that in adjacent normal lung tissues (3.3% [2/60]; $P < .01$; Table 1). Furthermore, the strongly positive rate of Paip1 protein expression in LADC was significantly higher in grade 3 (69.6% [16/23]) than that in grade 2 (32.3% [10/31]) and grade 1 (25.0% [1/4]; $P < .05$). Similarly, for TNM stage, the strongly positive rate of Paip1 protein expression in LADC was higher in advanced stage (III-IV[73.3% [11/15]) compared with that in early stage (I-II; 37.2% [16/43]; $P < .05$; Table 2, Fig. 1J and K). Moreover, Kaplan-Meier survival analysis showed that patients with high expression of Paip1 protein exhibited a lower rate of overall survival than did those with low Paip1 expression (log-rank = 6.893, $P = .009$; Fig. 1L). In summary, our clinical studies indicated that Paip1 was significantly overexpressed in LADC patients with poor prognosis.

3.2. Paip1 depletion attenuates the proliferation of A549 and H1299 lung cancer cells

To validate the role of Paip1, we detected the expression of Paip1 in 4 lung cancer cells. We found that A549 and H1299 cells were exhibited the highest protein levels of Paip1 (Fig. 2A). Thus, A549 and H1299 cell lines were used for control-siRNA and 3 different Paip1-siRNAs (siRNA1, siRNA2, and siRNA3) to knock down of Paip1 expression.

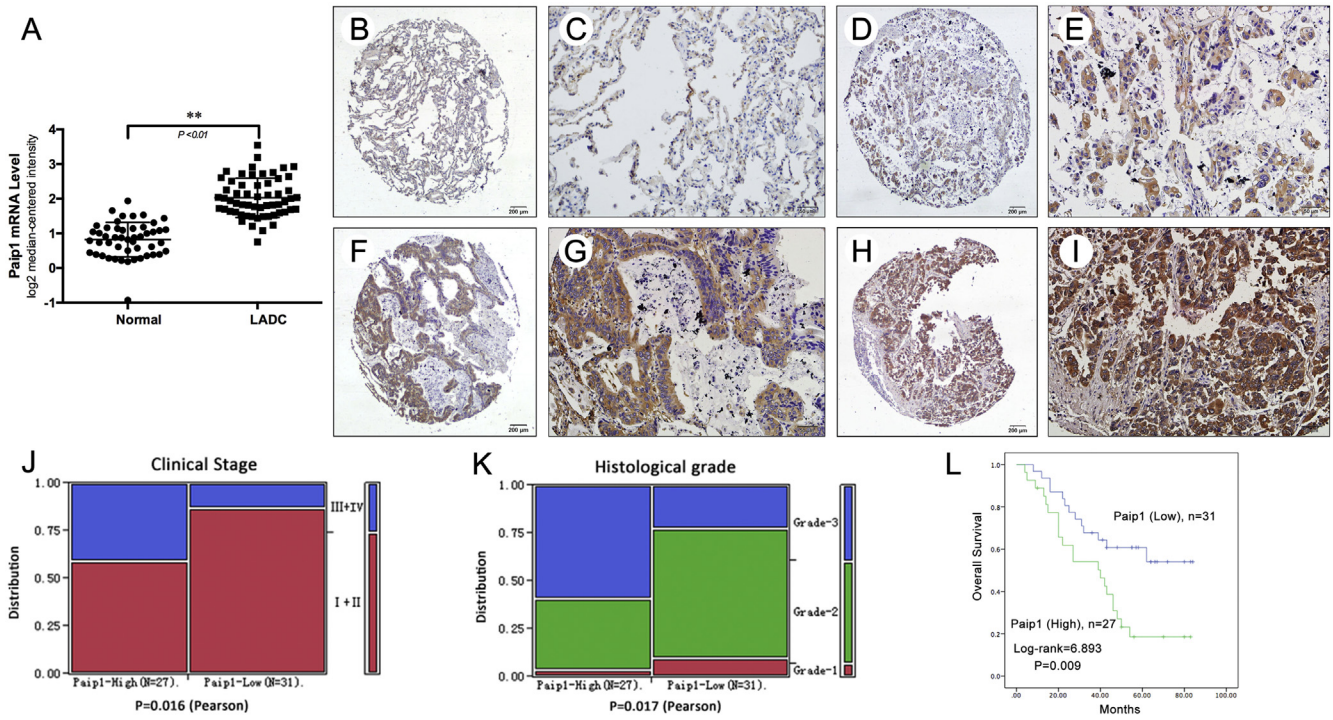

Fig. 1 Expression of Paip1 in LADC. A, Oncomine database showed that Paip1 mRNA level was higher in LADC tissues than in normal lung tissues. B and C, Negative Paip1 expression in adjacent normal lung tissue. D and E, Weak Paip1 expression in LADC tissue. F and G, Moderate Paip1 expression in LADC tissue. H and I, Strong Paip1 expression in LADC tissue. Panels C, E, G, and I indicated higher magnification of the selected area in panels B, D, F, and H, respectively. Original magnifications ×40 (B, D, F, and H) and ×200 (C, E, G, I). J and K, The expression level of Paip1 protein was significantly related with clinical stage (P = .016) and histologic grade (P = .017). L, Overall survival curves were significantly lower in patients with high (n = 27) Paip1 expression than in patients with low (n = 31) Paip1 expression.

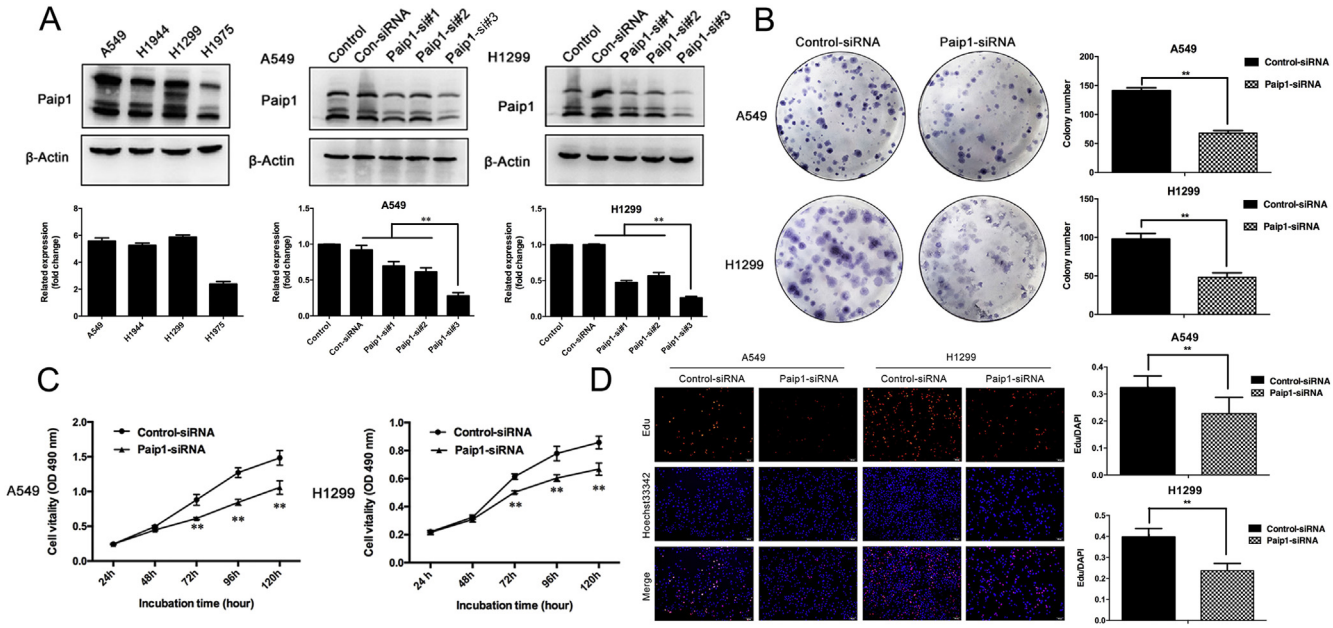

Fig. 2 Effect of Paip1 on A549 and H1299 lung cancer cell proliferation in vitro. A, The expression of Paip1 in lung cancer cell lines and knockdown of Paip1 in A549 and H1299 cells. B, Colony formation assays were used to determine the proliferation of Paip1-siRNA A549 and H1299 cells. Colonies were counted and captured. C, MTT assays were used to determine the viability of Paip1-siRNA A549 and H1299 cells. D, EdU staining assays were performed to determine the growth of Paip1-siRNA A549 and H1299 cells compared with the control-siRNA cells. *P < .05, **P < .01.

Among the analyzed siRNAs, siRNA3 seemed to have the greatest mean knockdown efficiency and was therefore selected for subsequent in vitro experiments (Fig. 2A). Next, colony formation and MTT assays showed that Paip1 depletion significantly attenuated the cell growth of A549 and H1299 cells (Fig. 2B and C). Moreover, EdU (red)/DAPI (blue) immunostaining also confirmed these results, Paip1 depletion significantly decreased the rate of cell proliferation (Fig. 2D). These data indicated that Paip1 depletion indeed inhibited the proliferation ability of A549 and H1299 lung cancer cells.

3.3. Paip1 depletion attenuates the migration of A549 and H1299 lung cancer cells

To further explore the effect of Paip1 on A549 and H1299 cell migration, wound healing and transwell assays were used to measure the migration ability. As shown in Fig. 3A and B, the data from the width of the wound revealed that Paip1 depletion inhibited the migration of A549 and H1299 cells. Furthermore, we assessed A549 and H1299 cell migration using transwell migration. As shown in Fig. 3C, Paip1 depletion also

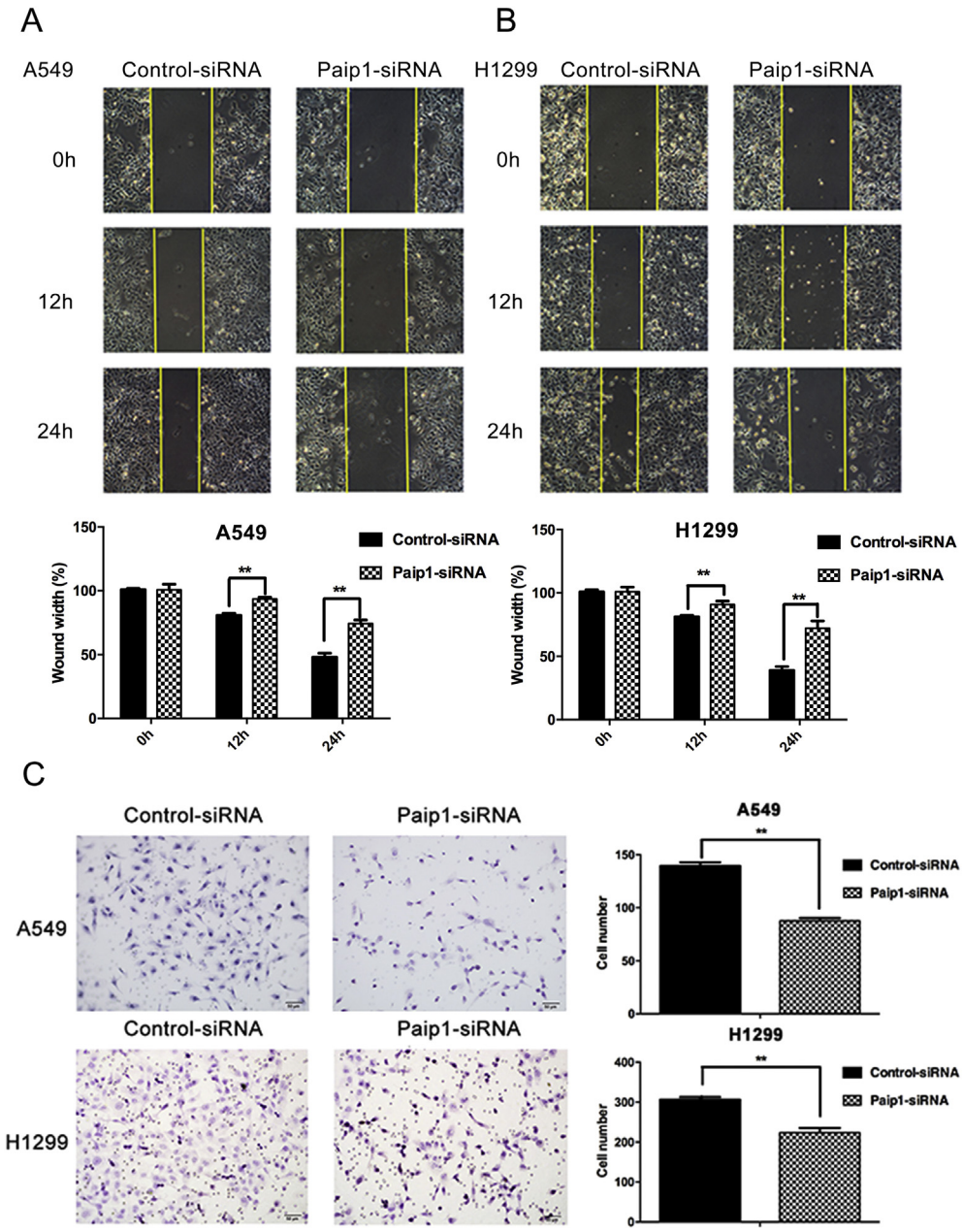

Fig. 3 Effect of Paip1 on A549 and H1299 lung cancer cell migration in vitro. A and B, Paip1 depletion inhibited migration ability of Paip1-siRNA A549 and H1299 cells compared with control-siRNA cells as determined by wound healing assay. Images were obtained at 0, 12, and 24 hours. C, Paip1 depletion inhibited migration ability of Paip1-siRNA cells compared with control-siRNA cells as determined by transwell assay. The number of cells that crossed the transwell membrane was counted. Original magnification ×200. *$P < .05$, **$P < .01$.

significantly reduced the migration ability of A549 and H1299 cells. These data indicated that Paip1 depletion attenuated cell migration potentials, suggesting an important role of Paip1 in lung cancer progression.

3.4. Paip1 regulates the expression of epithelial-mesenchymal transition–associated factors in A549 and H1299 lung cancer cells

To further study the underlying molecular mechanism of Paip1 in the regulation of cell migration, Western blot assay was performed to determine the expression of epithelial-mesenchymal transition (EMT)–related proteins. The results showed that Paip1-siRNA transfection downregulated mesenchymal marker vimentin and upregulated epithelial markers E-cadherin in A549 and H1299 cells. In addition, transcription factors Snail and Slug were decreased in Paip1-siRNA transfected cells compared with control-siRNA transfected cells (Fig. 4A). Next, we used immunofluorescence (IF) staining to examine the expression levels and localization of epithelial and mesenchymal markers in Paip1-siRNA and control-siRNA transfected cells. Consistent with the results of Western blot, downregulation of Paip1 significantly increased E-cadherin expression and decreased vimentin expression in A549 and H1299 cells (Fig. 4B). These suggested that Paip1 regulates the process of EMT in A549 and H1299 cells in vitro.

3.5. Paip1 regulates the EMT process of A549 and H1299 lung cancer cells through the AKT/GSK-3β signaling pathway

Previous studies showed that AKT signaling pathway was activated in many human carcinomas, and the AKT-driven EMT may confer the motility required for tumor cells invasion and metastasis [14]. To investigate which signaling pathway was affected by Paip1, Western blot assays was performed to evaluate the effect of Paip1 on the AKT/GSK-3β signaling pathway. Compared with the control-siRNA groups, we found that knockdown of Paip1 decreased the expression of phosphorylated AKT (Ser473) and GSK-3β (Ser9), whereas the expression of AKT

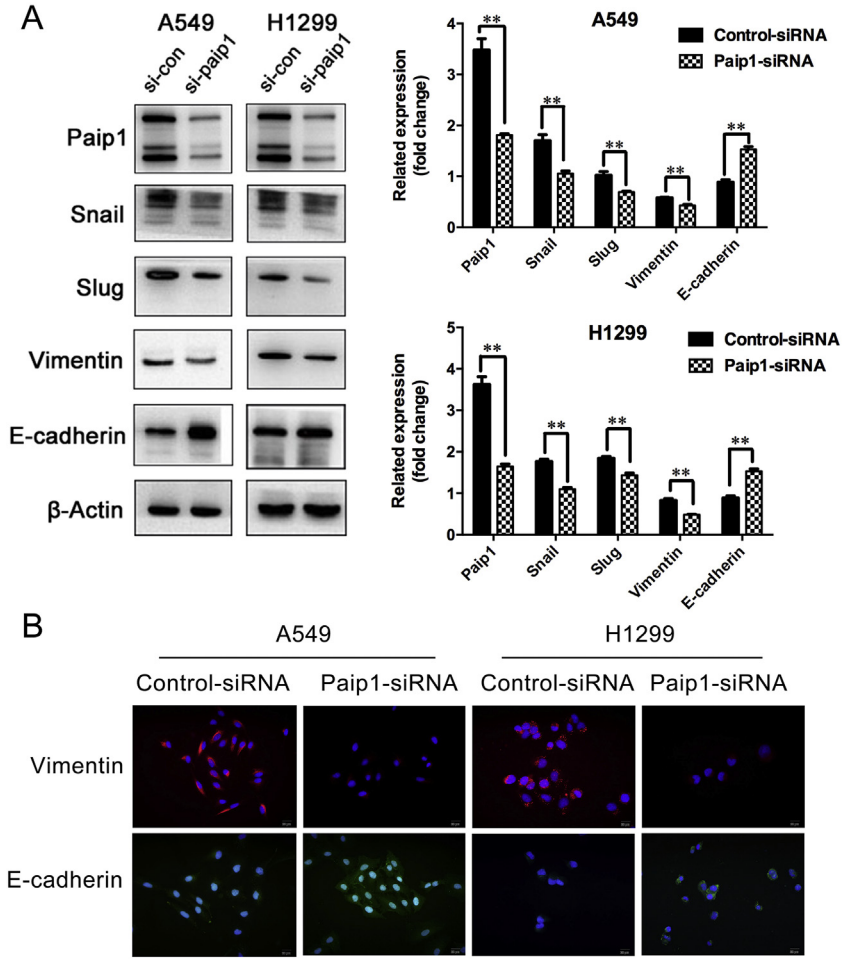

Fig. 4 Paip1 regulates the expression of EMT-associated factors in A549 and H1299 lung cancer cells. A, Western blot analysis of EMT markers in A549 and H1299 cells transfected with Paip1-siRNA and control-siRNA. β-Actin was used as a loading control. B, Expression of EMT markers was detected by IF staining in A549 and H1299 cells transfected with Paip1-siRNA and control-siRNA. *$P < .05$, **$P < .01$.

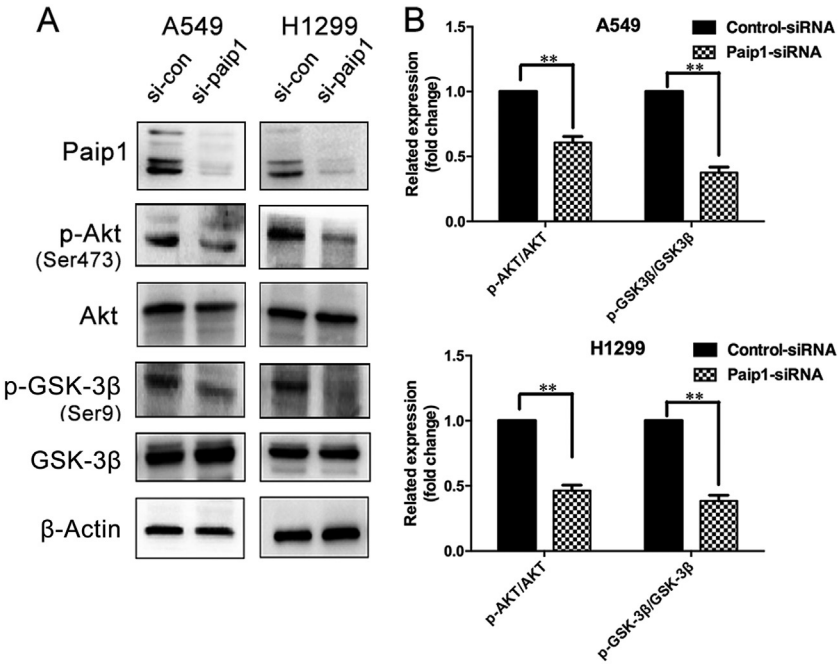

Fig. 5 Paip1 regulates the AKT/GSK-3β signaling pathway in A549 and H1299 lung cancer cells. A and B, Expressions of GSK-3β, p-GSK-3β, p-Akt, and Akt protein were determined in A549 and H1299 cells transfected with Paip1-siRNA and control-siRNA. β-Actin was used as a loading control. *$P < .05$, **$P < .01$.

and GSK-3β remained unchanged (Fig. 5A and B). Collectively, the results indicate that attenuated Paip1 expression suppresses A549 and H1299 cell proliferation and migration by regulating the AKT/GSK-3β signaling pathway.

4. Discussion

In eukaryotes, regulation of gene expression occurs during mRNA translation, specifically at the beginning of translation. Deregulation at this step of the translation process, the gene expression tends to be abnormal, which in the opposite way alters cell growth and even worse leads to cancer development [15-17]. Paip1 is a 479-amino-acid protein binds to PABP in vitro and in vivo and acts as a translational enhancer [18]. Grosset et al [19] reported that as a vital part of protein complex, Paip1 played an important role in mRNA turnover that stabilized the c-*fos* proto-oncogene mRNA by combining the major protein-coding-region determinant of instability. Lv et al [20] reported that overexpression of WWP2 significantly decreased the amount of Paip1 protein as a result of WWP2-mediated ubiquitin degradation, which meant that we can affect the level of Paip1 by regulating the amount of WWP2, so as to regulate the process of translation, as some Paip1-related diseases play a certain therapeutic effect.

For the first time, this study demonstrated that Paip1 mRNA levels were significantly increased in LADC tissues using microarray data from Oncomine database. Next, IHC staining of Paip1 protein expression was significantly upregulated in 77.6% LADC tissues, which significantly correlated with high histologic grade and advanced clinical stage. Importantly, we found that Paip1 overexpression correlated with poor survival of LADC patients. Besides these researches, upregulation of Paip1 was also found to predict poor prognosis in breast cancer [11]. These data suggested that Paip1 could serve as a potential oncoprotein and a predicting factor for poor survival LADC patients.

Cell proliferation as a consequence of cell cycle progression is the key process that leads to clonal expansion of initiated cells during tumor promotion [21]. Piao et al [11] showed that Paip1 depletion can significantly inhibit breast cancer cell proliferation and led to cell cycle arrest in the S phase and G_2/M phase. Similar with these results, knockdown of Paip1 expression attenuated A549 and H1299 cell growth and proliferation. Furthermore, tumor metastasis, a process of forming a new tumor in another part of the body, involves cell attachment, migration, and invasion [22]. Thus, one of the most important steps for cancer therapy might be inhibiting cancer cell metastasis. We further determined the role of Paip1 in A549 and H1299 cell motility by wound healing and migration assays. We found that Paip1 depletion markedly reduced the migration abilities of A549 and H1299 cells. Therefore, these data suggested that Paip1 might play an important role in LADC development and progression.

During lung carcinogenesis, normal lung epithelial cells undergo malignant transformation through an undefined etiology and mechanism. Moreover, accumulating evidence shows that NSCLC progression may involve tumor EMT to promote tumor cell invasion and metastasis [23,24]. In the present study, we explored that knockdown of Paip1 inhibited the migration ability underlying mechanism. Western blot and IF staining showed that

Paip1 depletion significantly increased E-cadherin expression and decreased vimentin expression in A549 and H1299 cells. This suggests that Paip1 could be a novel promoter of EMT process in A549 and H1299 cells. In addition, previous studies have reported that several key transcription factors that are called EMT-TFs including Snail and Slug [25] drive epithelial-originated malignancies going through EMT, leading to the dissociation of cancer cells from the primary sites to the distance [26]. Our results showed that Paip1 depletion reduced Snail and Slug expression in A549 and H1299 cells, suggesting that Paip1 regulates EMT process.

AKT pathway was widely acceptable as an enhancer of several cancer behaviors, including cancer metastasis [14]. We examined whether the AKT pathway was a target of the Paip1 that regulates EMT process. Western blot analysis demonstrated that AKT phosphorylation was strikingly decreased in A549 and H1299 cells with Paip1 depletion, whereas total AKT was unchanged. Recent evidence has suggested that AKT is able to influence the activity of GSK-3β [27,28]. In our research, the ratio of GSK-3β phosphorylation to GSK-3β was clearly diminished in A549 and H1299 cells with Paip1 depletion. These results are similar to the findings of the study by Derry et al [29] in which Paip1 contributed to increased translation in the cell by AKT-mTOR and the MEK signaling pathways. Hence, these results indicated that Paip1 regulated the AKT/GSK-3β signaling pathway in A549 and H1299 lung cancer cells.

In conclusion, our findings showed that Paip1 was significantly upregulated in LADC tissues and positively correlated with poor prognosis in LADC patients. Furthermore, Paip1 depletion significantly inhibited proliferation and EMT-related migration by regulating the AKT/GSK-3β signaling pathway in A549 and H1299 cells. Our research might provide a new perspective for Paip1 representing as a target for LADC diagnosis and treatment.

Author contributions

Zhenhua Lin and Tiefeng Jin conceived this study and takes responsibility for the quality of the data. Junjie Piao and Qianrong Wang participated in the tissue sample selection and experiments. Xuelian Cui and Ziqi Meng acquired data and played an important role in interpreting the results. Yixuan Wang performed the data analysis and wrote the manuscript. All authors read and approved the final manuscript.

CRediT authorship contribution statement

Yixuan Wang: Formal analysis, Investigation, Methodology, Writing - original draft. **Junjie Piao:** Data curation. **Qianrong Wang:** Data curation. **Xuelian Cui:** Supervision. **Ziqi Meng:** Validation. **Tiefeng Jin:** Conceptualization, Funding acquisition. **Zhenhua Lin:** Conceptualization, Funding acquisition, Writing - review & editing.

References

[1] Chen W, Sun K, Zheng R, et al. Cancer incidence and mortality in China, 2014. Chin J Cancer Res 2018;30:1-12.

[2] Siegel R, Ma J, Zou Z, et al. Cancer statistics, 2014. CA Cancer J Clin 2014;64:9-29.

[3] Ettinger DS, Akerley W, Bepler G, et al. Non–small cell lung cancer. J Natl Compr Canc Netw 2010;8:740-801.

[4] Herbst RS, Heymach JV, Lippman SM. Lung cancer. N Engl J Med 2008;359:1367-80.

[5] Yoshida BA, Sokoloff MM, Welch DR, et al. Metastasis-suppressor genes: a review and perspective on an emerging field. J Natl Cancer Inst 2000;92:1717-30.

[6] Gray NK, Coller JM, Dickson KS, et al. Multiple portions of poly(A)-binding protein stimulate translation in vivo. EMBO J 2000;19:4723-33.

[7] Craig AW, Haghighat A, Yu AT, et al. Interaction of polyadenylate-binding protein with the eIF4G homologue PAIP enhances translation. Nature 1998;392:520-3.

[8] Martineau Y, Derry MC, Wang X, et al. Poly(A)-binding protein-interacting protein 1 binds to eukaryotic translation initiation factor 3 to stimulate translation. Mol Cell Biol 2008;28:6658-67.

[9] Scotto L, Narayan G, Nandula SV, et al. Integrative genomics analysis of chromosome 5p gain in cervical cancer reveals target over-expressed genes, including Drosha. Mol Cancer 2008;7:58.

[10] Fukada Y, Yasui K, Kitayama M, et al. Gene expression analysis of the murine model of amyotrophic lateral sclerosis: studies of the Leu126-delTT mutation in SOD1. Brain Res 2007;1160:1-10.

[11] Piao J, Chen L, Jin T, et al. Paip1 affects breast cancer cell growth and represents a novel prognostic biomarker. Hum Pathol 2018;73:33-40.

[12] Edge SB, Compton CC. The American Joint Committee on Cancer: the 7th edition of the AJCC cancer staging manual and the future of TNM. Ann Surg Oncol 2010;17:1471-4.

[13] Mitsudomi T, Steinberg SM, Nau MM, et al. p53 gene mutations in non–small-cell lung cancer cell lines and their correlation with the presence of ras mutations and clinical features. Oncogene 1992;7:171-80.

[14] Grille SJ, Bellacosa A, Upson J, et al. The protein kinase Akt induces epithelial mesenchymal transition and promotes enhanced motility and invasiveness of squamous cell carcinoma lines. Cancer Res 2003;63:2172-8.

[15] Parsyan A, Hernández G, Meterissian S. Translation initiation in colorectal cancer. Cancer Metastasis Rev 2012;31:387-95.

[16] Jia Y, Polunovsky V, Bitterman PB, et al. Cap-dependent translation initiation factor eIF4E: an emerging anticancer drug target. Med Res Rev 2012;32:786-814.

[17] Graff JR, Konicek BW, Carter JH, et al. Targeting the eukaryotic translation initiation factor 4E for cancer therapy. Cancer Res 2008;68:631-4.

[18] Roy G, De Crescenzo G, Khaleghpour K, et al. Paip1 interacts with poly (A) binding protein through two independent binding motifs. Mol Cell Biol 2002;22:3769-82.

[19] Grosset C, Chen CY, Xu N, et al. A mechanism for translationally coupled mRNA turnover: interaction between the poly(A) tail and a c-fos RNA coding determinant via a protein complex. Cell 2000;103:29-40.

[20] Lv Y, Zhang K, Gao H, et al. Paip1, an effective stimulator of translation initiation, is targeted by WWP2 for ubiquitination and degradation. Mol Cell Biol 2014;34:4513-22.

[21] Zhong ZQ, Song MM, He Y, et al. Knockdown of Ezrin by RNA interference reverses malignant behavior of human pancreatic cancer cells *in vitro*. Asian Pac J Cancer Prev 2012;13:3781-9.

[22] Makrilia N, Kollias A, Manolopoulos L, et al. Cell adhesion molecules: role and clinical significance in cancer. Cancer Invest 2009;27:1023-37.

[23] Zeisberg M, Neilson EG. Biomarkers for epithelial-mesenchymal transitions. J Clin Invest 2009;119:1429-37.

[24] Bartis D, Mise N, Mahida RY, et al. Epithelial-mesenchymal transition in lung development and disease: does it exist and is it important? Thorax 2014;69:760-5.
[25] Nieto MA, Huang RY, Jackson RA, et al. EMT: 2016. Cell 2016;166:21-45.
[26] Zhang Y, Zhang X, Ye M, et al. FBW7 loss promotes epithelial-to-mesenchymal transition in non–small cell lung cancer through the stabilization of Snail protein. Cancer Lett 2018;419:75-83.
[27] Lee K, Nelson CM. New insights into the regulation of epithelial-mesenchymal transition and tissue fibrosis. Int Rev Cell Mol Biol 2012;294:171-221.
[28] Shih JY, Yang PC. The EMT regulator slug and lung carcinogenesis. Carcinogenesis 2011;32:1299-304.
[29] Derry MC, Yanagiya A, Martineau Y, et al. Regulation of poly(A)-binding protein through PABP-interacting proteins. Cold Spring Harb Symp Quant Biol 2006;71:537-43.